NONEQUILIBRIUM STATISTICAL MODELS: GUIDED NETWORK GROWTH UNDER LOCALIZED INFORMATION AND PERSPECTIVES ON ELECTRON DIFFUSION IN CONDUCTORS

by

ALEXANDER J. TREVELYAN

A DISSERTATION

Presented to the Department of Physics
and the Graduate School of the University of Oregon
in partial fulfillment of the requirements
for the degree of
Doctor of Philosophy

March 2018

DISSERTATION APPROVAL PAGE

Student: Alexander J. Trevelyan

Title: Nonequilibrium Statistical Models: Guided Network Growth Under Localized Information and Perspectives on Electron Diffusion in Conductors

This dissertation has been accepted and approved in partial fulfillment of the requirements for the Doctor of Philosophy degree in the Department of Physics by:

Benjamin McMorran	Chair
Eric Corwin	Advisor
Daniel Steck	Core Member
Michael Pluth	Institutional Representative

and

Sara D. Hodges	Interim Vice Provost and Dean of the Graduate School

Original approval signatures are on file with the University of Oregon Graduate School.

Degree awarded March 2018

DISSERTATION ABSTRACT

Alexander J. Trevelyan

Doctor of Philosophy

Department of Physics

March 2018

Title: Nonequilibrium Statistical Models: Guided Network Growth Under Localized Information and Perspectives on Electron Diffusion in Conductors

The ability to probe many-particle systems on a microscopic level has revolutionized the way we do statistical physics. As computational capabilities continue to grow exponentially, larger and more complex systems come within reach of microscopic analysis. In the field of network growth, the classical model has given way to competitive processes, in which networks are guided by some criteria at every step of their formation. We develop and analyze a new competitive growth process that permits intervention on growing networks using only local properties of the network when evaluating how to add new connections. We establish the critical behavior of this new method and explore potential uses in guiding the development of real-world networks.

The classical system of electrons diffusing within a conductor similarly permits a microscopic analysis where, to date, studies of the macroscopic properties have dominated the literature. In order to extend our understanding of the theory that governs this diffusion—the fluctuation-dissipation theorem—we construct a physical model of the Johnson-Nyquist system of electrons embedded in the bulk of a conductor. Constructing the model involves deriving how the motion of each individual electron comes about via scattering processes in the conductor, then connecting this collective motion to the macroscopic observables that define Johnson-Nyquist noise. Once the equilibrium properties have been fully realized, an external perturbation can be applied in order to probe the behavior of the model as it deviates away from equilibrium. In much the same way that competitive network growth revolutionized classical network theory, we establish a model which can guide future research into nonequilibrium fluctuation-dissipation by providing a method for interacting with the system in a precise and well-controlled manner as it evolves over time.

Chapter II has been published in *Physical Review E* as a Rapid Communication [1]. The writing and analysis were performed by me as the primary author. Eric Corwin and Georgios Tsekenis are listed as co-authors for their contribution to the analysis and for advisement on the work.

This dissertation includes previously published co-authored material.

CURRICULUM VITAE

NAME OF AUTHOR: Alexander J. Trevelyan

GRADUATE AND UNDERGRADUATE SCHOOLS ATTENDED:

University of Oregon, Eugene, OR
Loyola Marymount University, Los Angeles, CA

DEGREES AWARDED:

Doctor of Philosophy, Physics, 2018, University of Oregon
Bachelor of Science, Engineering Physics, 2009, Loyola Marymount University

AREAS OF SPECIAL INTEREST:

Soft Condensed Matter
Network Theory
Statistical Mechanics

PROFESSIONAL EXPERIENCE:

Research Assistant, Physics, University of Oregon, 2011-2018

GRANTS, AWARDS AND HONORS:

Sigma Xi Research Society, Loyola Marymount University, 2009

Sigma Pi Sigma Honor Society, Loyola Marymount University, 2009

PUBLICATIONS:

A. J. Trevelyan, G. Tsekenis, E. I. Corwin. "Degree product rule tempers explosive percolation in the absence of global information." *Phys. Rev. E* **97**, 020301(R) (2018).

J. Sanny, D. Berube, A. Trevelyan, B. Sorbom, P. Amy. "Storm-time fingerprints and global profiles of ULF wave power at geosynchronous orbit." *Planet. Space Sci.* **57**, 2087 (2009).

ACKNOWLEDGEMENTS

First and foremost, I would like to thank my wonderful family—my parents, Yvonne and Ian, and my sister Alyssa. I would not have made it here without them. The guidance of my graduate advisor, Eric Corwin, was instrumental in helping me navigate my way to this point and grounding me as a scientist and critical thinker. He's the real The Boss, sorry The Boss (Bruce Springsteen). Additionally, I'd like to thank all of my labmates over the years, in particular Peter, Yasin, Kyle, and Andy for our many productive conversations about Magic: The Gathering. And to everyone else who helped along the way, a list too long to properly enumerate, I am eternally grateful.

TABLE OF CONTENTS

LIST OF FIGURES

LIST OF TABLES

CHAPTER I

INTRODUCTION

We live in the age of computation. For my generation, our parents multiplied large numbers by sliding a marked piece of wood, averaging an operation per second, perhaps two for the deft of hand. Meanwhile, the invention of the solid-state transistor set in motion what surely has become the greatest increase in raw technological capability to this point in history, propelling our computational abilities from the order of one per second in the 1940s to a staggering 10^{13} operations per second in a single consumer brand GPU this year. It strains the mind to think of anything else that has even approached a similar scale of improvement in such a short period of time (and yet, even a moderate slowdown of our personal computer is now cause for major headache). The impact of this abrupt and dramatic proliferation in computing power has been felt across nearly all facets of modern society, and statistical physics is no exception. Prior to the transistor, statistical physicists relied on averaging the expected behavior of a system's constituents and working with the resulting distributions—one cannot expect to make much headway calculating one trajectory per second for billions of particles, or forming a network containing millions of nodes one connection at a time. However, we now suddenly find ourselves with the power to do exactly that, and with it the ability to explore systems that resist the type of coarse-grained approach necessitated by classical equilibrium statistical mechanics.

Perhaps the first thing that jumps to mind for statistical physicists excited by this newfound computing power is the ability to enumerate large swaths of configurational space. In this sense, computation won a symbolic victory in 1996, when Deep Blue scored its first win over reigning chess world champion Garry Kasparov by brute-force analyzing 100 million positions per second, making it abundantly clear that the human brain's finesse with pattern recognition and approximately 100 billion neurons each firing once per second, on average, could no longer keep up with the burgeoning microprocessor. Ironically, in the intermediating time, further increases in computing power have led us right back to the human brain, with AlphaZero attaining the highest chess Elo rating (the most common chess rating system, developed by Arpad Elo) ever by using reinforcement learning on deep convolutional neural networks [2].

If the deep exploration of configurational space can be thought of as the unpacking of *ensemble* averages in statistical mechanics, then the other natural frontier is to unpack the *time* averages. What exactly does this mean? In equilibrium, it might mean nothing at all. For example, holding the relevant state variables constant, measuring the properties of one container of an ideal gas at many different snapshots in time will produce identical results to measuring many separate containers, each holding an identical ideal gas, all at the exact same moment. These are the time averages and ensemble averages, respectively. The time average is obtained by observing a single system at different points in time, assuming variables such as volume, pressure, and temperature have all remained constant across the observations. Conversely, the ensemble average is obtained by observing many identical copies of a system, with the same state variables held constant across every system. Now imagine separate rooms with either one container (time average), or a collection of identical containers (ensemble average) spread throughout, have heating vents to keep the poor graduate student warm, producing a steady temperature gradient from one end of each room to the other. The first case with a single container might not notice this at all, having simply equilibrated to the temperature wherever it sits in the room. The second case with many containers, however, will produce a more complicated result that takes into account the distance of each container from the heater and its corresponding temperature. Apply the same logic to a separate situation with perfectly uniform temperature throughout each room but faulty, fluctuating thermostats and we can see how unpacking the two types of averaging give us unique insights into *nonequilibrium* systems.

The work that follows focuses on systems driven out of equilibrium in the time domain, in the sense that a statistical system is prepared at some initial time, then is continuously interacted with in some way while it evolves. In other words, rather than existing within a static environment, the system is subject to perturbations that drive its evolution over time. For example, imagine the look of shock on Deep Blue's face if you decided at some point in the middle of a chess game that the functionality of the chess pieces was to change—that a rook now moved like a queen. Kasparov might initially be befuddled as well, but there is no doubt he would adapt to the new rules and march forward with more than a semblance of strategy. Alternatively, its wealth of chess tables and all the computational power in the world to search them would not help Deep Blue make use of the rook's newfound power. This type of dexterity is an inspiration for

modelling physical systems driven out equilibrium in the time domain, affording us the power to deftly interact and keep up with complex systems as they evolve within our modern civilization, marching us forward with some semblance of strategy. Toward this end, the following chapters first introduce a new scheme for intervening on growing networks, using an edge evaluation method we call the *degree product rule process*. Next, we develop a time-dependent ground-up model of one of the most fundamental results in statistical mechanics, Johnson-Nyquist noise [3].

As the modern world continues to become ever more interconnected, understanding how statistical systems evolve in time is more consequential than ever. The financial crisis that began in 2007 exposed the fragility of the interbank loan networks that went into upheaval and quickly spread a cascade of default across the entire financial system. The relatively fast pace of the growth of the internet in the 1990s became dwarfed even more quickly by social networks in the 2000s, as data floods servers faster than it can be parsed and analyzed. Air travel networks now transport more people in a year than lived on Earth fifty years ago, and sudden disruptions at large airports can be catastrophic to the movement of passengers in a timely manner. Each of these examples have at their core a statistical framework that dictated the system's evolution over time, which to varying degrees we could exert control over as each one came to fruition, and most of which were prone to forces that drove them far from any notion of equilibrium. A more guided and nimble approach to our treatment of these systems in the future could prove instrumental in improving their capability to help modern civilization function in the manner we've come to expect.

In Chapter II, we explore a new process of competitive network growth, demonstrating that interventions during the formation of networks can have far-reaching effects on the critical properties of the percolation phase transition. The ability to continually intervene on large networks as they grow requires immense computational power, as the evaluation criteria must be computed at each step, and the number of steps grows with network size as N^2, where N is the size of the network. Chapter II has been published in *Physical Review E* [1] as a Rapid Communication. The writing, experimental design, and analysis were performed by me as the primary author. Eric Corwin and Georgios Tsekenis are listed as co-authors for this work and aided in the analysis of the critical properties of the networks. Chapter III tackles the intricacies of recreating a famous experimental result from first principles by modelling electron diffusion

in a conductor. In order to test the resiliency of the fluctuation-dissipation theorem [4, 5] in nonequilibrium systems, we design a foundational model for Johnson-Nyquist noise that allows fine control over how the system is driven out of equilibrium. Constructing this simulation requires tracking the movement of many particles, and can only approximate the behavior of a physical conductor for increasing number of electrons. The work in Chapter III is unpublished at this time.

Both chapters share the principle of exploring the time evolution of statistical systems driven away from equilibrium. Each is a model of a physical process with well-understood macroscopic, equilibrium properties that layed the groundwork for major advances in statistical mechanics during the 20th century. In both cases, we rebuild the model from the ground up, providing the experimenter the ability to precisely control how the system is driven away from equilibrium and measure the response of the system to perturbations of varying form and magnitude. We hope that both models can serve as a launching point for similar types of studies in the future.

CHAPTER II

DEGREE PRODUCT RULE TEMPERS EXPLOSIVE PERCOLATION IN THE ABSENCE OF GLOBAL INFORMATION

This chapter has been published in *Physical Review E* as a Rapid Communication [1]. The writing and analysis were performed by me as the primary author. Eric Corwin and Georgios Tsekenis are listed as co-authors for their contribution to the analysis and for advisement on the work.

Abstract

We introduce a guided network growth model, which we call the degree product rule process, that uses solely local information when adding new edges. For small numbers of candidate edges our process gives rise to a second-order phase transition, but becomes first-order in the limit of global choice. We provide the set of critical exponents required to characterize the nature of this percolation transition. Such a process permits interventions which can delay the onset of percolation while tempering the explosiveness caused by cluster product rule processes.

Background

Network-based approaches continue to see growing applications in a wide array of fields, from epidemiology [6, 7] to finance [8, 9], neuroscience [10, 11], and machine learning [12]. As we increasingly rely on networks, understanding how they form out of complex conditions becomes all the more consequential [13–17]. Many of the networks we entrust to support our modernized society—transportation, financial, social, etc.—are formed with some amount of agency, meaning that potential new members have control over how they connect and interact with the network. This agency can lead to markedly different behavior compared to the classical case of purely random network growth [18]. In particular, networks subject to competitive edge addition break time-reversal symmetry, as there is no well-defined method for running the process in reverse that achieves a statistically identical growth curve [19]. Furthermore, edge competition can be used as a means of control over cluster growth and connectivity within a growing network. Depending on the desired outcome (delayed connectivity for contagion spreading, increased connectivity

for communication networks, etc.), intervening on growing networks can help produce more specialized and responsive networks.

Pioneering work by Erdős and Rényi [20] characterized the most straightforward process of random network growth: edges are added to the network uniformly at random until connectivity *percolates* through the entire network. The Achlioptas growth process (AP) [21] adds a layer of competition to the classical percolation process, whereby edges are ranked based on the sizes of the clusters they join and then added to the network in such a way as to suppress large cluster growth. This competition results in a significant delay in the onset of percolation, but comes at the cost of a much more abrupt transition—it produces what is commonly referred to as "powder keg" conditions [22, 23], where clusters in a narrow band of size become widespread and primed for sudden connectivity. The powder keg formation can be mitigated by continuously adding new nodes to the network [24, 25], inducing an infinite-order transition; however, in many real-world cases such an intervention is impractical.

Variations in competitive edge addition, such as the minimal cluster rule [23], the triangle rule [26], and a handful of others covered in the review article in reference [27], achieve results similar to the AP. Together, these growth processes are referred to as *explosive percolation* due to the abruptness with which the largest cluster grows from microscopic to system-spanning. Each of these processes shares a common thread: edge competition involves comparing the sizes of the clusters to which each edge belongs, which necessitates gathering information about the connectivity of a large portion of the network as it nears the percolation threshold. Although generally second-order [19], under certain circumstances these transitions can become first-order [28], typically when either the number of edges competing for addition at each timestep grows quickly enough with system size [29], or the competition process is designed to build up smaller clusters that eventually merge together and overtake the largest component [30]. Approaches focused on local measures of connectivity [31, 32] have reproduced some aspects of explosive percolation, yet remain relatively unexplored compared to global product rules. Additional novel phenomena that have been observed in explosive percolation including crackling noise and "fractional percolation" [33], unexpected double-peaked distributions of the order parameter in small systems [34], and finite-size hysteresis [35].

Here, we introduce and characterize the behavior of a third type of random growth process, the *degree product rule* (DPR) process. Mechanistically, the DPR is analogous to the Achlioptas process, the difference being that the criteria used to evaluate edges is the product of node degrees (the number of edges attached to a node) rather than cluster sizes. The impetus for studying such a subtle but fundamental modification is twofold. First, the degree of a node is local information in the sense that for any given node, determining its degree requires only knowledge of its set of nearest neighbors. Unlike average cluster size, information about the average degree of each node does not become extensive within the system near the percolation threshold. Second, the problem of classical percolation has long involved using a stable probability distribution to choose an edge at each timestep. Explosive percolation upended this notion by allowing the distribution to shift unpredictably depending on which edge is chosen, a characteristic potentially more in line with how certain types of real networks take shape [36]. The DPR similarly produces unpredictable changes when updating edge selection probabilities, but does so under a set of local rules, broadening our understanding of how networks coalesce under various formational pressures.

The Degree Product Rule Model

We begin with a fully disconnected set of N nodes and successively add edges one at a time, such that at time t the network contains exactly t edges, with a resulting edge density $p = t/N$. The growth process is as follows: 1) A specified number of candidate edges m are chosen uniformly at random. 2) The weight of each candidate edge is calculated as the product of the degrees d of the two nodes to be connected by that edge as $(d_1 + 1)(d_2 + 1)$, where one is added to the degree of each node in order to avoid the degenerate case of zero-degree nodes. 3) The edge with the smallest weight is added to the network or, in the case of a tie, an edge is chosen at random from the set of edges with the smallest weight. The remaining edges are discarded back into the pool of unfilled edges. The process is illustrated diagrammatically in the inset of Figure 1.

During any random growth process clusters will form, grow, and eventually merge together. The relative size of the largest cluster C/N is computed at every timestep and serves as the order parameter of the percolation transition. The order parameter begins vanishingly small, then becomes macroscopic as the system crosses the critical point p_c, the precise value of which is determined by the details of the growth process. Figure 1 shows the ensemble-averaged evolution

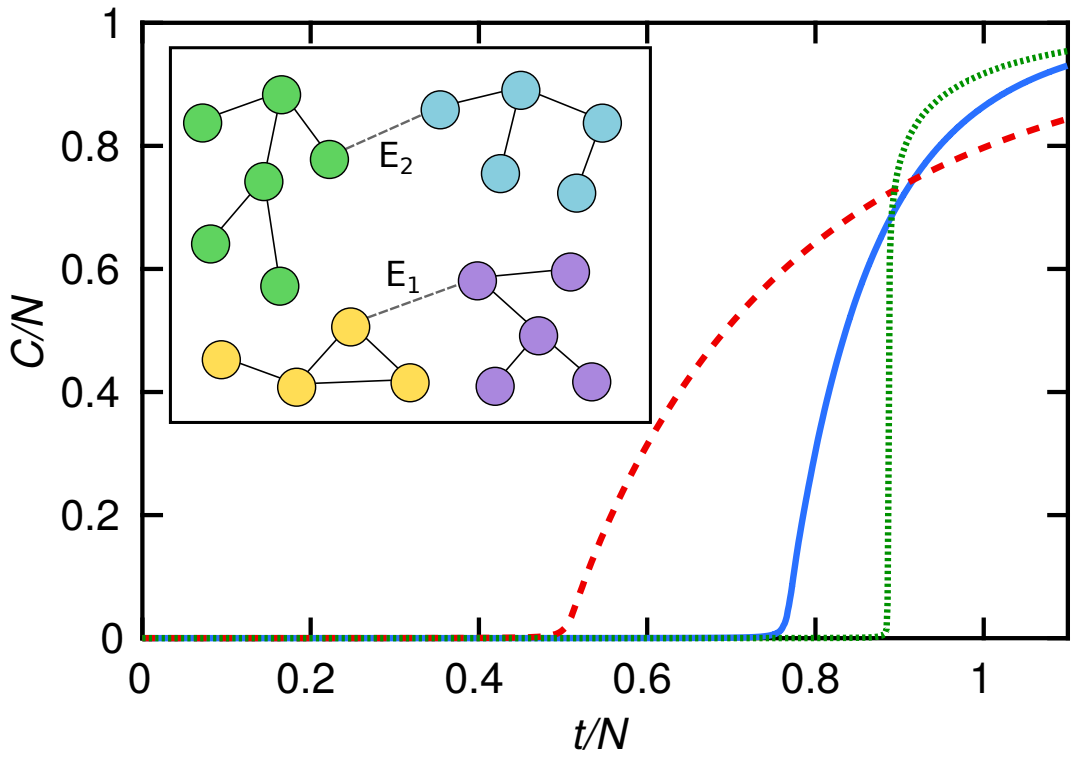

FIGURE 1. Degree product rule scheme and evolution of the largest cluster.
Relative size of the largest cluster, C/N, at scaled time $p = t/N$. Ensemble averages for Erdős-Rényi (dashed red), DPR process (solid blue), and AP (dotted green) at $N = 3.6 \times 10^5$ nodes and $m = 2$ choices for the DPR process and AP. Inset: Example of the DPR selection scheme for $m = 2$ choices. E_1 and E_2 compete for addition. The selection criteria $A = (d_1 + 1)(d_2 + 1)$ is computed for each edge. Since $A_{E_1} = 9$ and $A_{E_2} = 4$, E_2 is added to the network.

of the order parameter for the Erdős-Rényi, Achlioptas, and DPR processes, with $m = 2$ for the latter two. In principle, the critical point of each transition can be predicted by analyzing the combinatorics of the system, however in practice this becomes prohibitively difficult when the underlying distribution used to add edges changes unpredictably as in the AP and DPR. Thus, numerical simulations are necessary to tackle the details of these systems and obtain precise approximations of their critical behavior.

The percolation transitions presented in Figure 1 are notably different in both the location of the critical point and the abruptness of each transition. To better quantify the abruptness of the DPR transition, we measure the size of the largest jump in the order parameter $\Delta C_{max}/N$ during each realization, then average over many realizations. This type of convergence criterion is common among explosive percolation studies [37–40], as it gives insight into how the transition

behaves in the thermodynamic limit and indicates whether the transition is first- or second-order. For increasing system size, the largest jump will decay as a power law when the transition is second-order, $\Delta C_{max}/N \sim N^{-\omega}$, whereas if there is a discontinuity that survives in the thermodynamic limit then $\Delta C_{max}/N$ will approach a constant value, signaling that the transition is first-order. The decay exponent ω communicates the level of the abruptness in second-order transitions, with smaller values indicating a sharper transition. In the AP, the decay exponent is unusually small: $\omega = 0.065$ for $m = 2$ choices. The DPR, however, produces decay exponents similar to Erdős-Rényi, as shown in Figure 2. In fact, despite the appearance of a faster transition, the DPR is actually seen to have a decay exponent only slightly larger than Erdős-Rényi, recorded in Table I. In addition, finite-size effects show up at small system sizes for the DPR between $N = 10^2$ up to $N = 10^4$ in Figure 2, depending on the number of choices, whereas in both Erdős-Rényi and explosive percolation no such effects appear at comparable system sizes.

Increasing the number of choices does not appear to change the decay exponent in the DPR process, unlike in the AP [37], which suggests that the locality of the information used in the DPR suppresses its ability to achieve the buildup of multiple large clusters that inevitably leads to bigger jumps in the order parameter. This is even more striking given that the value of the critical point increases from $p_c \approx 0.76$ for $m = 2$ choices to $p_c \approx 0.93$ for $m = 10$ choices and $p_c \approx 0.97$ for $m = 50$ choices, eventually asymptoting to $p_c \approx 1$ for global choice, implying that increasing the number of choices works to suppress the transition without actually building up the so-called powder keg conditions necessary to achieve explosiveness. Rather, the DPR works to constrict the degree distribution, as shown in Figure 3, which leads to something of a powder keg in the node degrees instead of cluster sizes. However, in contrast to explosive percolation, this degree-oriented powder keg does not "ignite" near the critical point.

Despite the lack of a powder keg, global choice in the DPR process nevertheless produces a first-order phase transition. We simulated global choice using the following process, as increasing the number of choices becomes computationally intensive at large system sizes. Initially, every node is randomly paired with another unpaired node, at which point the node pairs begin to join together and form chains. Only the two ends of each chain are candidates for edge addition, as they have degree $d = 1$ while internal nodes in the chain have degree $d = 2$. Eventually these chains will tend to form large, closed loops whenever the two ends of a single chain are

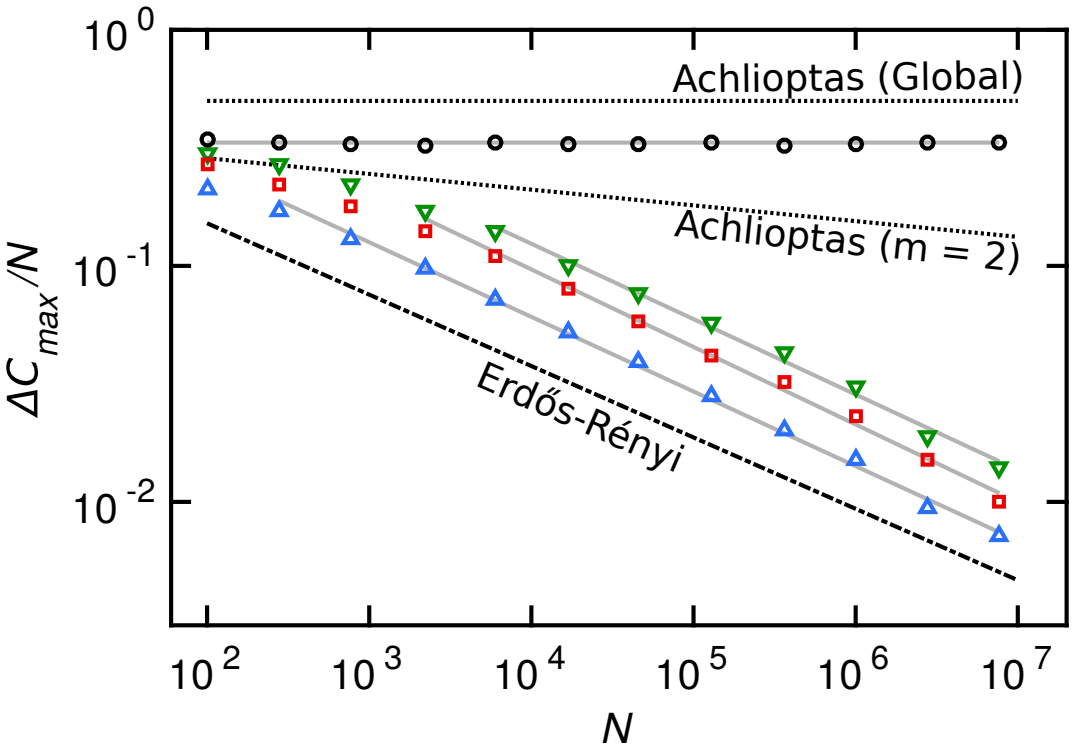

FIGURE 2. Maximum jump in the order parameter.
The average maximum jump in the order parameter as a function of system size for the DPR process with two choices (blue upward triangles), ten choices (red squares), fifty choices (green downward triangles), and global choice (black circles). Erdős-Rényi (lower dashed line), as well as the AP with two choices (lower dotted line) and global choice (upper dotted line) are shown for comparison. Fits to the data (gray lines) for the three non-global DPR processes have decay exponents of $\omega = 0.316$, $\omega = 0.328$, and $\omega = 0.319$, respectively.

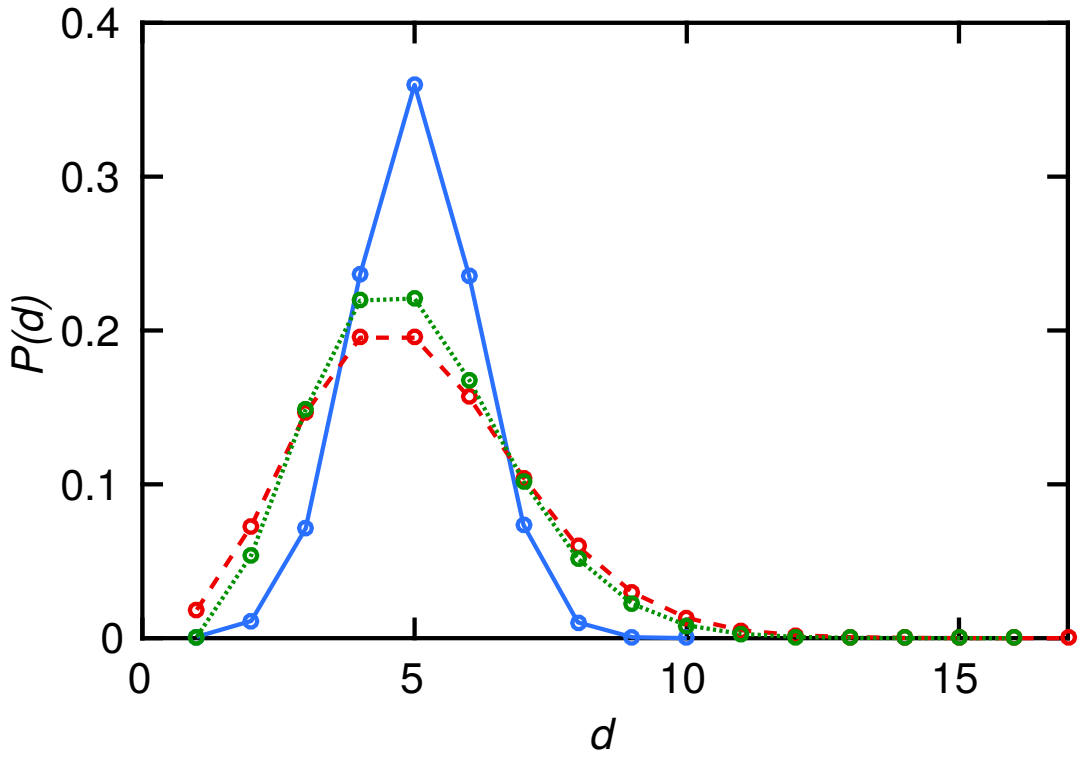

FIGURE 3. Degree distributions.
The degree distributions at $p = 5$ for Erdős-Rényi (dashed red), degree product rule process (solid blue), and Achlioptas process (dotted green) at $N = 1.7 \times 10^4$ nodes and $m = 2$ choices for the DPR process and AP.

randomly chosen to join together. The loops then merge together very close to $p = 1$, shortly after every node has degree $d = 2$, resulting in a critical point of $p_c \approx 1$ since the largest jump in the order parameter will tend to occur when two large loops merge. The result is a first-order phase transition with exclusively short-range information dictating its development. Similar to the AP with global choice, the largest jump for the DPR with global choice remains constant, with an approximate value of $\Delta C_{max}/N = 0.33$ for all N, shown in Figure 2. However, in the DPR process, the crossover from second-order to first-order appears to happen via the extension of a shoulder at increasing system sizes as the number of choices increases, rather than the typical rise in the slope of the power law seen in explosive percolation. Essentially, what appears to be finite-size effects observed with increasing number of choices could in fact be a signifier of a slow crossover to a discontinuous transition.

TABLE 1. Summary of critical exponents.

Critical point p_c, and summary of critical exponents for the three growth processes discussed in this paper with $m = 2$ for the AP and DPR processes.

Growth process	p_c	β/ν	γ/ν	τ	ω
Erdős-Rényi	0.5	0.33	0.34	2.5	0.3
DPR	**0.763**	**0.33**	**0.37**	**2.45**	**0.32**
Achlioptas	0.888	0.02	0.48	2.08	0.065

Criticality and Universality

Second-order phase transitions are characterized by critical behavior, which permits the use of scaling theory in determining universal behavior near the critical point [41, 42]. These functional forms are a result of the fact that all state variables associated with the phase transition behave as power laws near the critical point due to scale independence within the system. Using this process, one finds a rescaling of the order parameter for system size that has the following general form:

$$C = N^{-\beta/\nu} F[(p - p_c)N^{1/\nu}] \tag{2.1}$$

The value of β is associated with the behavior of the order parameter with system size, while ν scales the correlation length (mean distance between nodes in a cluster) with the distance to the critical point. The function F is a universal function that allows collapse onto a single master curve. The average cluster size S should rescale in a similar manner, although with a different critical exponent affecting the system size and a separate universal function H:

$$S = N^{\gamma/\nu} H[(p - p_c)N^{1/\nu}] \tag{2.2}$$

Here, the exponent γ scales the average cluster size (excluding the giant component) with system size N. Together, equations (1) and (2) contain the set of critical exponents and scaling functions required to characterize the DPR phase transition and allow universal collapse onto master curves. Measuring the critical exponents necessitates finding both the largest cluster size and the average size of clusters (excluding the largest) at the critical point for varying system sizes. The critical point serves as a separatrix for the largest cluster size—at the critical point it will follow a power law with growing system size, while above and below the critical point

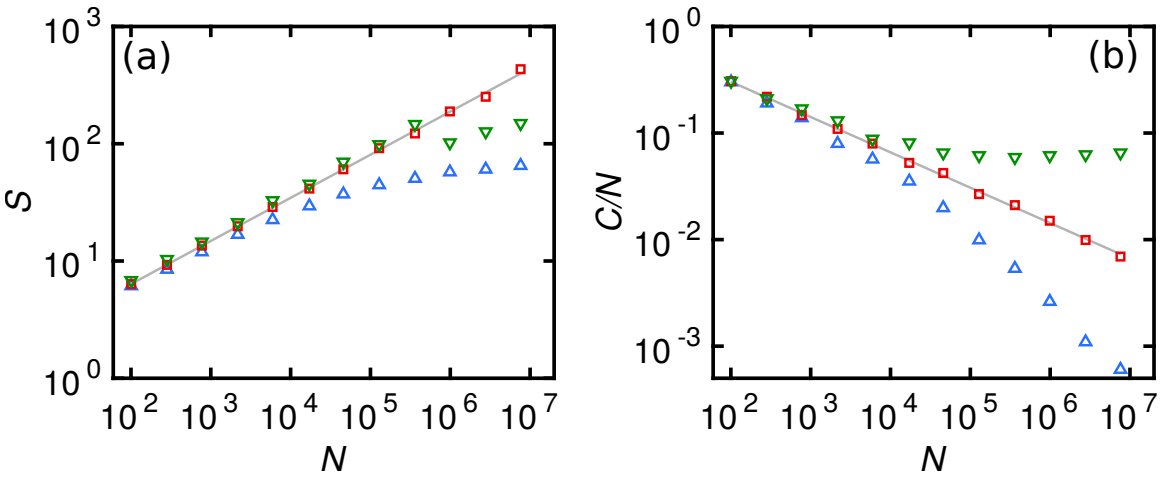

FIGURE 4. Finite-size scaling.
Finite-size scaling for the critical exponents β/ν and γ/ν of the DPR process. (a) Mean cluster size S is plotted versus system size N. The fit at $p = p_c = 0.763$ (red squares) gives the value $\gamma/\nu = 0.37$. (b) Relative size of the largest cluster C/N is plotted versus system size N. The fit at $p = p_c = 0.763$ (red squares) gives the value $\beta/\nu = 0.33$. Breakdown of the power law scaling away from the critical point is shown in both (a) and (b) for $p = 0.75$ (blue upward triangles) and $p = 0.77$ (green downward triangles).

it will increasingly curve away from the separating line due to the excess (or deficit) of edges interrupting the scale-free nature of the system. The average size of the remaining clusters, however, will decay with growing system size both above and below the critical point due to the largest cluster absorbing an increasing portion of the nodes above the critical point. Figure 4 illustrates this behavior, which provides an additional check on the approximate value of the critical point, $p_c = 0.763$. The fits in Figure 4a and 4b provide values of $\beta/\nu = 0.33$ and $\gamma/\nu = 0.37$, respectively, for the scaling exponents of the DPR process. Again, these values draw comparisons to the classical Erdős-Rényi process despite the fundamental differences in reversibility and information loss between the two growth processes.

Along with the set of critical exponents, the Fisher exponent τ, which describes the power law decay of the cluster size distribution at the critical point, completes the picture of how the network percolates. By revealing the structure of cluster sizes beyond the largest component, the Fisher exponent provides details about how susceptible the network is to forming larger clusters near the critical point. Shown in Figure 5, the cluster size distribution at the critical point follows the form $G(s) \sim s^{1-\tau}$. The decay in cluster size for the DPR process is well-fit by a power law with $\tau = 2.45$, which may be consistent with Erdős-Rényi ($\tau = 2.5$). The cluster size distributions

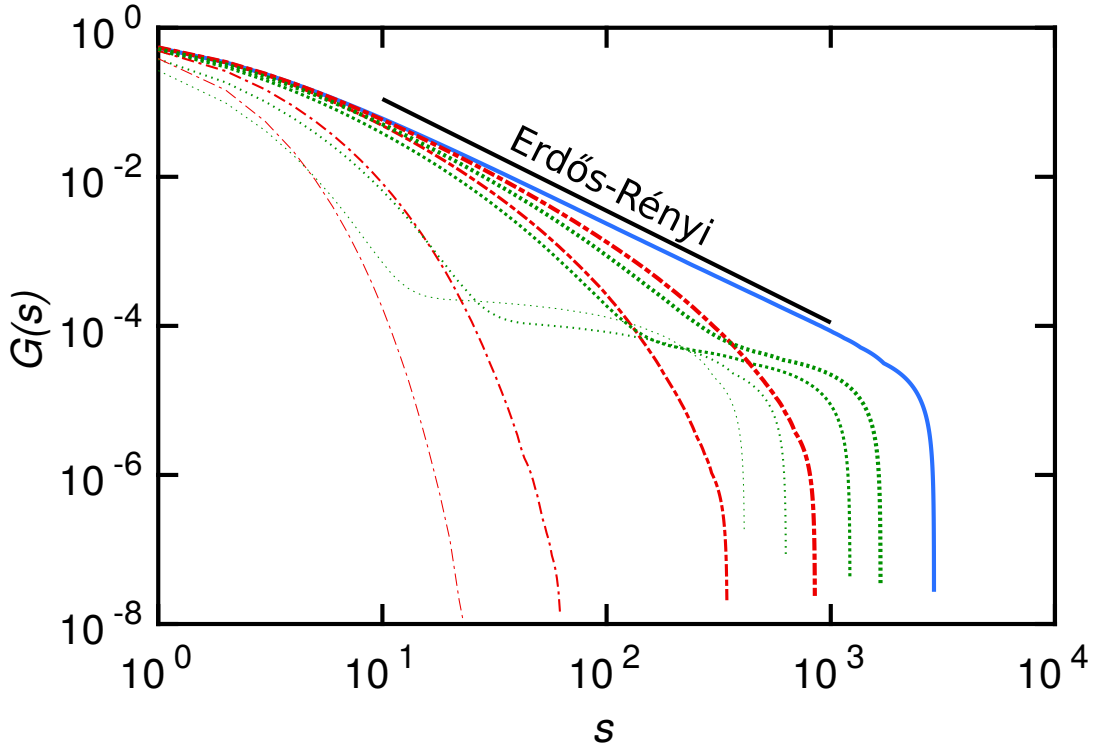

FIGURE 5. Cluster size distributions.
Cumulative distribution of cluster sizes at the critical point (solid blue) and at points above (green dotted) and below (red dot-dashed) the critical point for $N = 1.3 \times 10^5$ nodes. Thicker lines are nearer to the critical point. The solid black line is a guide for Erdős-Rényi ($\tau = 2.5$). The Fisher exponent, $\tau = 2.45$, is found by fitting a power law to the distribution at the critical point. Red dot-dashed curves are for $p = 0.38$, 0.46, 0.54, 0.62, green dotted curves are for $p = 0.92$, 1, 1.08, 1.15.

of the DPR process above the critical point show a mixture of explosive and classical behavior—plateaus form as in explosive percolation, however the distributions above the critical point remain entirely below the distribution at the critical point, as is the case in Erdős-Rényi growth [19]. This seems to suggest that the DPR process preferentially builds a few large clusters after the critical point, though it substantially delays building up the remaining smaller clusters as compared to explosive percolation. A comparison of the three growth processes considered in this paper is presented in Table 1.

Conclusions

Prescriptive processes for network growth, such as the one we presented, that tune percolation while circumventing the formation of a powder keg are useful in cases where connectivity is a liability. Here, we have described a way in which networks can be designed and grown that delays the onset of percolation without the risk of sudden connectivity, allowing for more manageable failure modes in cases where connectivity is undesirable. This growth scheme provides a set of tools for researchers in a wide array of fields to use when intervening on growing networks, requiring a great deal less information when making decisions about how to guide networks towards more desirable topologies. In cases where acting quickly on a developing network is crucial, the DPR can be enacted with ease whereas enacting cluster-oriented growth schemes may be impractical.

Our work establishes that in order to turn a percolation transition from second-order to first-order one need not necessarily have access to global information, as in explosive percolation. In addition, the use of local information extends the lower bound for explosive percolation to even lower critical connectivities than previously accessible with global information.

The selection criteria in DPR grown networks could be further altered in order to use the product of degrees of second-nearest, or third-nearest neighbors, etc., methodically extending the distance with which information about connectivity is communicated within a network. Such a tool could allow for improved modeling of networks where interactions extend to a finite distance. Degree rule processes may also be of interest within the context of core percolation [43], as they naturally produce networks with larger cores due to the narrow width of the degree distribution compared to traditional and explosive percolation.

CHAPTER III

MODELING NONEQUILIBRIUM FLUCTUATION-DISSIPATION THEOREM IN AN ELECTRON GAS

Abstract

The observation of equilibrium fluctuations of voltage and electrical current in a conductor provided a path to the very first formulation of the fluctuation-dissipation theorem, which states that for small perturbations to equilibrium, a statistical system cannot tell the difference between the perturbation and a random fluctuation. Here we attempt to build a foundational model of the Johnson-Nyquist system of charge carries diffusing in a conductor, first aiming to recreate this seminal result, then providing a course to a more detailed analysis of nonequilibrium states and deviations from equilibrium fluctuation-dissipation theorem in driven systems. By accounting for the relevant physical phenomena, an agent-based statistical model could allow simultaneous measurement of the two fundamental quantities in the fluctuation-dissipation relation, providing insight into how thermodynamic systems experience nonequilibrium states continuously over a single period of time.

Background

For over 250 years the state of the art in statistical mechanics involved calculating the properties of distributions created by a system's constituent particles, then predicting the macroscopic behavior of the system from the moments of these distributions. The development of the kinetic theory of gases [44] refined our understanding of how macroscopic quantities such as pressure and temperature are connected to the molecular underpinnings of a system, while simultaneously underlining the relative impossibility of tracking the evolution of the system on a microscopic level. In equilibrium, when there is no active exchange of energy with the surrounding environment—or equivalently, when the entropy is a concave function of the state variables [45]—the classical approach of working with distributions works exceedingly well. However, the further a system moves from equilibrium, the more difficult it becomes to extract meaningful results as the distributions of state variables evolve in complex ways over time and the entropy no longer resides in a global minimum.

Over the course of the 20th century physicists steadily incorporated nonequilibrium dynamics into equilibrium models, extending our understanding of statistical thermodynamics to *near-equilibrium systems*. Einstein's famous paper on Brownian motion [46] helped build the framework for investigating near-equilibrium systems by describing the mathematical process of diffusion and the resulting average particle density in fluids. This involved quantifying particle distributions for systems in dynamical equilibrium (e.g. in equilibrium but with a spatially uniform potential) and accounting for dissipation of energy through drag. One of the most impactful observations about near-equilibrium statistical systems is the idea, formulated by Harry Nyquist in 1928 [3], that small external perturbations are experienced by a system identically to a random thermal fluctuation originating within the system itself. This idea is known broadly as the fluctuation-dissipation theorem, and successfully describes a wide variety of equilibrium noise processes [47, 48].

More recently, apparent violations of the fluctuation-dissipation theorem in nonequilibrium systems [49, 50] have spurred interest in the development of a more generalized theorem for treating perturbations that drive a system far from equilibrium. Efforts to extend the fluctuation-dissipation relation to nonequilibrium systems include adjusting the Langevin dynamics for a particle in a periodic potential [51], defining an *effective temperature* for a sheared fluid [52], or expanding around small variations in a system's control parameters for nonequilibrium steady states [53]. The work that follows complements these approaches by building a model system from the ground up, rather than perturbing an existing equilibrium system and attempting to correct for its deviations from equilibrium. The primary advantage of building a foundational model is to allow for finer control over how perturbations are introduced, tracking the response of systems as they deviate further from equilibrium by using the strength of the perturbing potential as an experimental parameter.

Developing the Model

The model system we have chosen to use in order to probe nonequilibrium fluctuation-dissipation is the Johnson-Nyquist noise produced by a conductor. Within a conductive material at finite temperature, some fraction of charge-carrying particles are unbound and free to diffuse within the bulk of the conductor. Although energy conservation requires that the time-averaged

flow of current from these free particles must be zero, at any given time a nonzero current will be measured when two electrodes are connected across the conductive material, regardless of any applied voltage. This phenomenon was observed in solid-state resistors by J.B. Johnson in 1928 [54] and accounted for theoretically by Harry Nyquist [3] in the same year. Thus, when averaged over long times, a piece of conductive material with finite resistance and at finite temperature will produce a fluctuating voltage (and, necessarily, current) that obeys a Gaussian distribution with zero mean. The variance of the Gaussian distribution of voltages, however, depends on the temperature and resistance of the conductor in the following way:

$$\overline{V^2} = 4k_B T R \tag{3.1}$$

This is the primary result of Johnson's and Nyquist's analysis of fluctuations in an equilibrium conductor. Larger resistance, or a higher ambient temperature, will generate stronger voltage fluctuations, with the associated variance in electrical current via Ohm's Law:

$$\overline{I^2} = 4k_B T / R \tag{3.2}$$

The fluctuating voltage and electrical current are each assumed *uncorrelated* in time, meaning that any observation is unaffected by previous measurements, and so for sufficiently low frequencies the fluctuations are well-modeled by Gaussian distributed white noise. Any model we develop in order to explore fluctuation-dissipation must first be capable of reproducing these established voltage and current fluctuations described by Johnson and Nyquist. Towards this end, we must be able to simulate our system of diffusing electrons and from it extract measurements of voltage and current over long periods of time, building distributions for each that match the properties defined above. We accomplish this by considering the microscopic properties of the conductor and building up a picture of how they contribute to the macroscopic properties observed in Johnson-Nyquist noise. Following Kittel [55], we begin by connecting the total voltage across the conductor to the contribution of each individual charge carrier:

$$V = IR = \rho A e \overline{u} R \tag{3.3}$$

Where A is the cross-sectional area of the resistor, ρ the number of charge carriers N per unit volume, e the charge of an electron, and $\overline{u}$ the average drift velocity of the particles, such that the current flowing in the resistor $I = \rho A e \overline{u}$ is the average drift velocity of the N particles multiplied by the electron charge and the cross-sectional area of the conductor. The voltage is measured across opposite ends of the conductor, which we idealize as a cylinder. From here we note that $\rho A l \overline{u} = \sum_i u_i$, where l is the length of the conductor, and each u_i is a random variable that assigns a drift velocity to each particle. This suggests that the voltage at any given time is the summation of the random voltages contributed by each charge carrier,

$$V = (eR/l) \sum_i u_i = \sum_i V_i \tag{3.4}$$

This simple but powerful observation is the crux of the model. If the fluctuating voltage has as its source the random motion of the charge carriers, then the macroscopic behavior should be recoverable from the ensemble average of the particles' motion. At a snapshot in time, assuming an idealized cylindrical conductor with length $l \gg r$, where r is the radius of the cross-sectional area A, the voltage is well-approximated by the summation of every particle's difference in location from the left and right side of the cylinder. The contribution to the total voltage from each particle is then the difference in potential felt by the left and right surface of the conductor:

$$V = e/4\pi\epsilon_0 \sum_i \left(\frac{1}{x_i} - \frac{1}{l - x_i} \right) \tag{3.5}$$

The model of the conductor, along with the quantities required in order to calculate the voltage, are illustrated in Figure 6. In order to implement this model, we need to know how the particles diffuse within the conductor. Solid-state theory suggests that for a pure conductor at a finite temperature, at any given time a portion of electrons will contain sufficient energy to reside in the conduction band. These electrons can be well-approximated as a gas of free particles freely diffusing in the bulk of the conductor, described in detail by Sommerfeld and Bethe [56] as the *free electron model*. What remains at this point is to determine the mechanisms by which these free electrons scatter as they diffuse within the conductor.

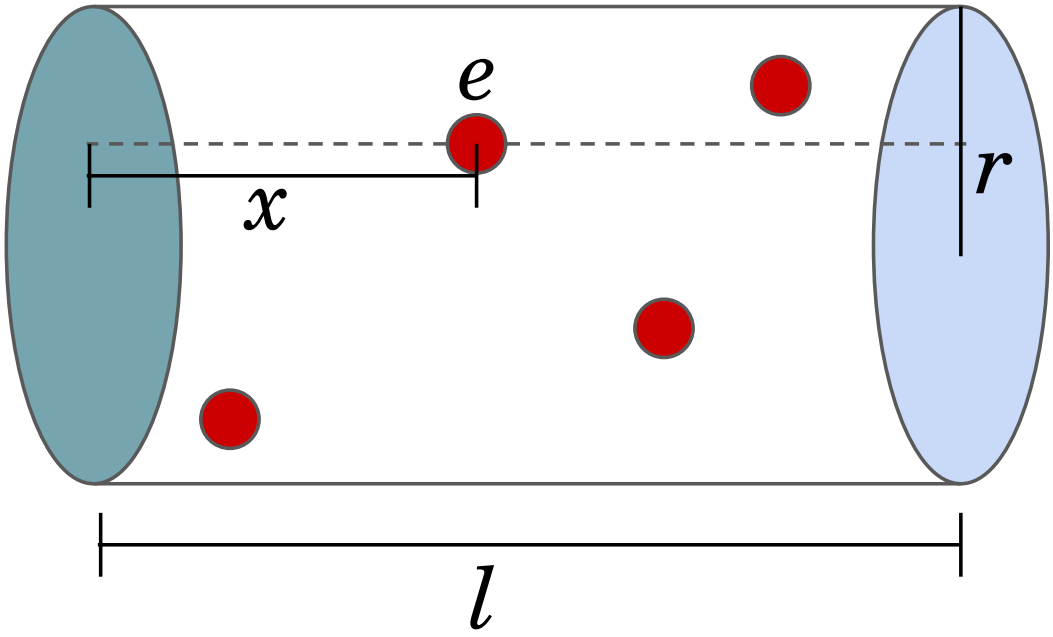

FIGURE 6. Diagram of the model conductor
A diagram of the conductor showing embedded electrons (red circles) with charge e. The length of the conductor l is indicated, as well as the cross-sectional radius r and distance x from the left surface (positive) electrode.

Scattering Mechanisms in the Electron Gas

In low-resistivity conductors, electrons will tend to move in ballistic trajectories through free space until they encounter a scattering mechanism. Depending on the details of the system, scattering mechanisms can include other electrons, lattice impurities and defects, and phonons, to name a few of the most common processes in conductors. The contribution to the overall scattering cross-section can be calculated from Matthiessen's Rule [57], which states that the drift mobility of the free electrons is,

$$1/\mu = \sum_i 1/\mu_i \tag{3.6}$$

Where μ is the total average mobility of electrons in the gas and each μ_i is the mobility contributed by each scattering mechanism. More appropriate in this case is to discuss the contribution of each scattering element to the *mean free path* of the electrons, which is the average distance traveled before encountering a scattering mechanism. As the mean free path

is proportional to the mobility, it too obeys Matthiessen's Rule, $1/\lambda = \sum_i 1/\lambda_i$, where λ_i is the mean free path afforded by each scattering mechanism.

The primary scattering mechanism in conductors depends on the ambient temperature as well as the material properties of the conductor. For most conductors, however, the phonon-electron interaction begins to dominate above the Debye temperature, which for many common metals is below room temperature [58]. As such, we choose the temperature regime for our simulations well into the Debye phase, and consider electron-phonon scattering as the sole scattering process. Consequently, the mean free path of the electrons can be derived from the probability per unit time of a collision with a phonon, which depends directly on the phonon density in the conductor.

Between collisions, the electrons reside on a Fermi surface in three-dimensional momentum space [59], and each collision with a phonon shifts the electron to a new point on the Fermi surface. In an idealized conductor, the Fermi surface is simply a sphere, such that the electrons maintain a constant momentum at all times. When an electron is scattered, it moves to a new location on the Fermi surface chosen uniformly at random.

The simulation proceeds according to the following steps: 1) A specified number of electrons are deposited uniformly at random inside the conductor, with velocity vectors of equivalent magnitude but random direction in three-dimensional space. 2) Each electron moves ballistically for a distance specified by a single realization of an exponentially distributed random number with mean equal to the mean free path of the electrons in the conductor. 3) When an electron has moved the distance afforded to it by its free path, it scatters off of a phonon, drawing a new direction uniformly at random and a new free path from the specified exponential distribution.

Defining an Electrical Current

In the simulation, we impose periodic boundary conditions on the electrons. The conductor, then, has a defined length, and the electrons which move beyond this length are assumed to travel through the abstracted current measurement device with no resistance before immediately re-entering the conductor on the opposite side. In our initial design, each electron that passes through the boundary contributes one unit of current—positive if the electron moves through from

the right side of the boundary and negative if it moves through from the left. Summing the total contributions from every electron that passed through the boundary in a specified period of time gives the electrical current measurement at each point in time as,

$$I_t = \Delta Q / \Delta t \tag{3.7}$$

Where each electron passing the boundary contributes either $+Q$ or $-Q$ to ΔQ, the total count. A curiosity arises from this definition: the electrical current, which is simply proportional to voltage via Ohm's Law, depends on a measurement over a time interval, whereas the voltage is an instantaneous measurement. In other words, the voltage contains no information about how the system evolved between measurements, while the current is entirely defined by that evolution. When measuring electron flow from an applied voltage, this nuance is easily attributed to shot noise, as the applied voltage typically dwarfs the contribution from any particular electron to the overall voltage, and the fluctuations from the discrete nature of the electrons is negligible when comparing the flow of current to the applied voltage. However, in the Johnson-Nyquist system with zero applied voltage, effects typically attributed to shot noise become prominent.

The time series of voltage and current measurements should behave like a *Markov process*, which is a *memoryless* evolution between states in the sense that future measurements are independent of all past measurement, or, more specifically, that the transition probability between states depends only on the current state of the system. If this property holds, then the time series of measured voltage and current will follow the experimentally observed *Gaussian white noise*. Gaussian white noise is uncorrelated, resulting in a constant power across all frequencies (up to a critical frequency), and follows a Gaussian distribution in the limit of many measurements. Measurements of the current under the counting scheme introduced above, however, appear to contain a memory element under the conditions of the simulation.

The reason that a memory appears to form in the electrical current measurements is due to the relative timescales of scattering and electron mobility compared to the length of the conductor. For a sufficiently long conductor, the measurement of a crossing in one direction carries with it an increasing probability that a crossing in the opposite direction will occur within a short time, based on how long it takes for the electron to move within range of crossing again in the same direction. In other words, there is a decay time after measuring a crossing for which the

electron cannot move quickly enough to cross again in that direction, while staying within range of crossing backwards if it scatters in the opposite direction soon after crossing the boundary. Thus, a memory of the electrical current is formed, with a decay time that depends on electron mobility, scattering rate, and length of the conductor. Each electron carries with it the memory of its last crossing for a time defined by these three factors, indicating a decaying likelihood of contributing the opposite value in future measurements. This manifests itself by allowing the observer to predict more probable measurements of the opposite sign (positive versus negative) based on how large the current previously fluctuated in one direction and how long the observer waited between measurements. The process is no longer uncorrelated, and instead produces peaks in the power spectrum of fluctuations.

If the model is to reproduce the current fluctuations observed in physical observations of the Johnson-Nyquist system, the memory problem must be addressed. Although there are likely a variety of potential resolutions, one straightforward method for making the process memoryless is to make the measurement continuous rather than a discrete counting process. To accomplish this, the electrical current would be determined according to,

$$I_t = \sum_i \Delta x_i / \Delta t \tag{3.8}$$

Where each electron contributes to the current based on the distance traveled in a particular direction along the length of the conductor. When measuring current this way, information about how the electron moved in any previous timestep is discarded once the measurement is made, and its displacement is tracked anew starting from the point it occupied at the time of the last measurement.

In equilibrium, the mean free path of each electron depends only on the temperature of the system. For increasing temperature, a higher phonon density results in an increased probability per unit time that an electron will scatter to a new point in momentum space, thus reducing the mean free path of the electrons. Figure 7 illustrates how the current fluctuations depend on the mean free path, demonstrating that an increase in temperature—which correlates with a decrease in mean free path—will cause larger fluctuations. The relationship between temperature and mean free path can be extracted by tracking the variance of the Gaussian fits. Figure 8 shows

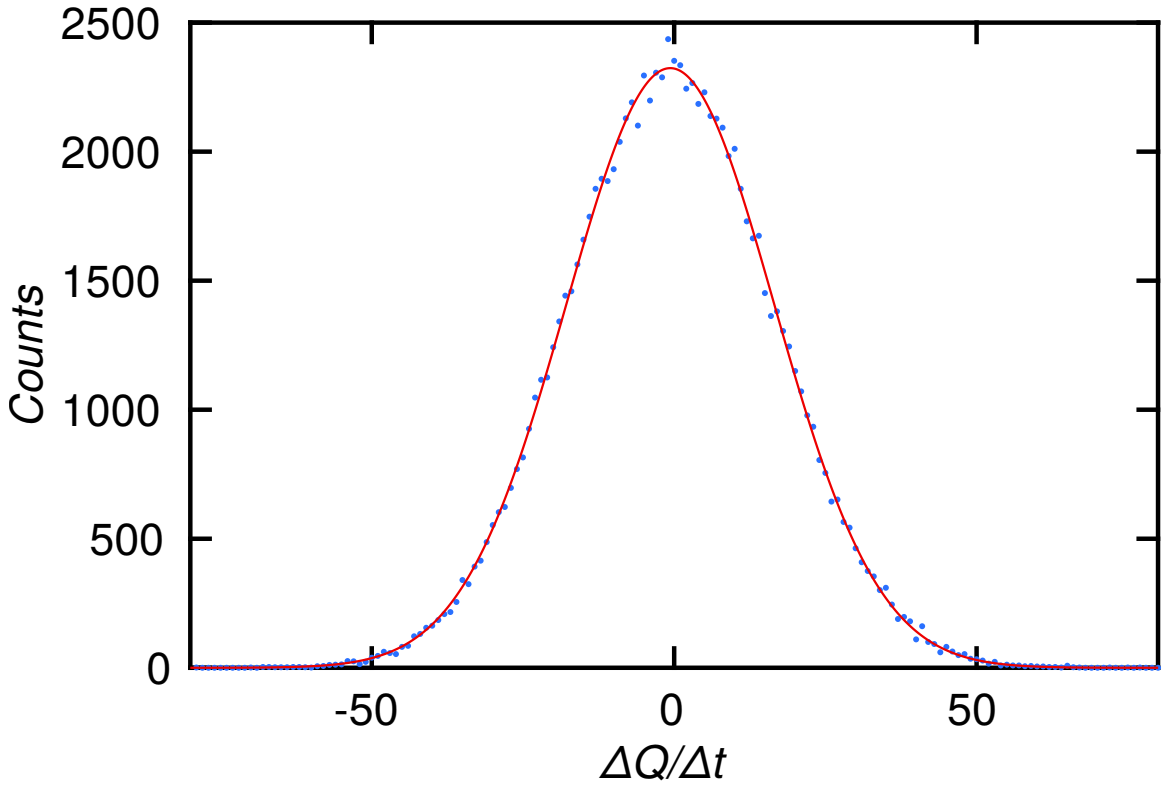

FIGURE 7. Equilibrium fluctuations of the electrical current
Electrical current fluctuations in the model conductor fit to a Gaussian for $\lambda = 1$. Blue dots are data, while the red line is a Gaussian fit with $\mu = -0.64$ as the mean and $\sigma = 24.3$ as the standard deviation.

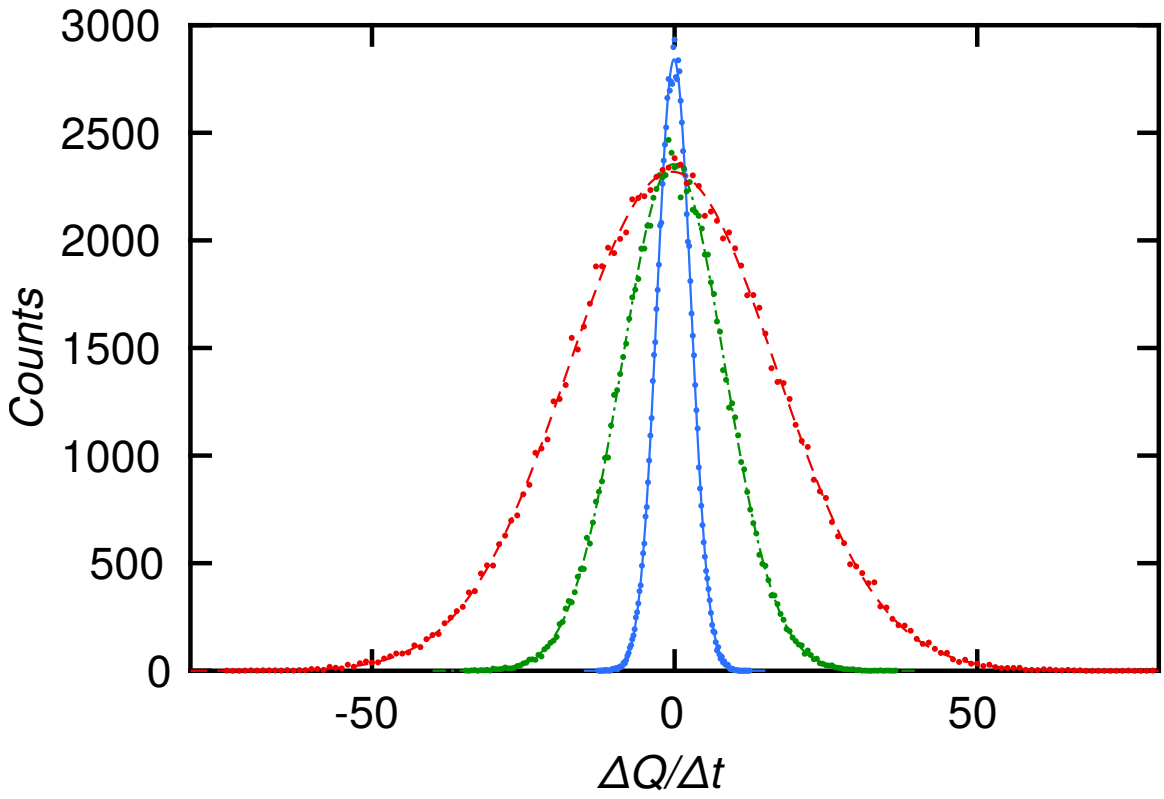

FIGURE 8. Temperature dependence of current fluctuations in equilibrium
Electrical current fluctuations in the model conductor fit to Gaussians for varying temperature. The mean free path of electrons is varied in each curve, with blue $\lambda = 0.01$, green $\lambda = 0.1$, and red $\lambda = 1$.

the variance of electrical current fluctuations as a function of mean free path, which is closely approximated as a linear relationship for mean free path below $\lambda \approx 1$.

The dependence of the variance of fluctuations on temperature shown in Figure 8 is unexpected given our understanding of the underlying physics and construction of the model. For increasing temperature, the variance of current fluctuations increase via the Johnson-Nyquist relation $\overline{I^2} = 4k_BT/R$. Higher temperature also means an increase in the phonon density, causing more scattering events per unit time and decreasing the mean free path of the electrons. Thus, we would expect a shorter mean free path to result in larger current fluctuations, which is not the case. Instead, Figure 8 demonstrates that the current fluctuations *increase* for larger value of the mean free path. Clearly, there are additional physical phenomena that must be taken into account, otherwise the underlying physics of the model must be reevaluated.

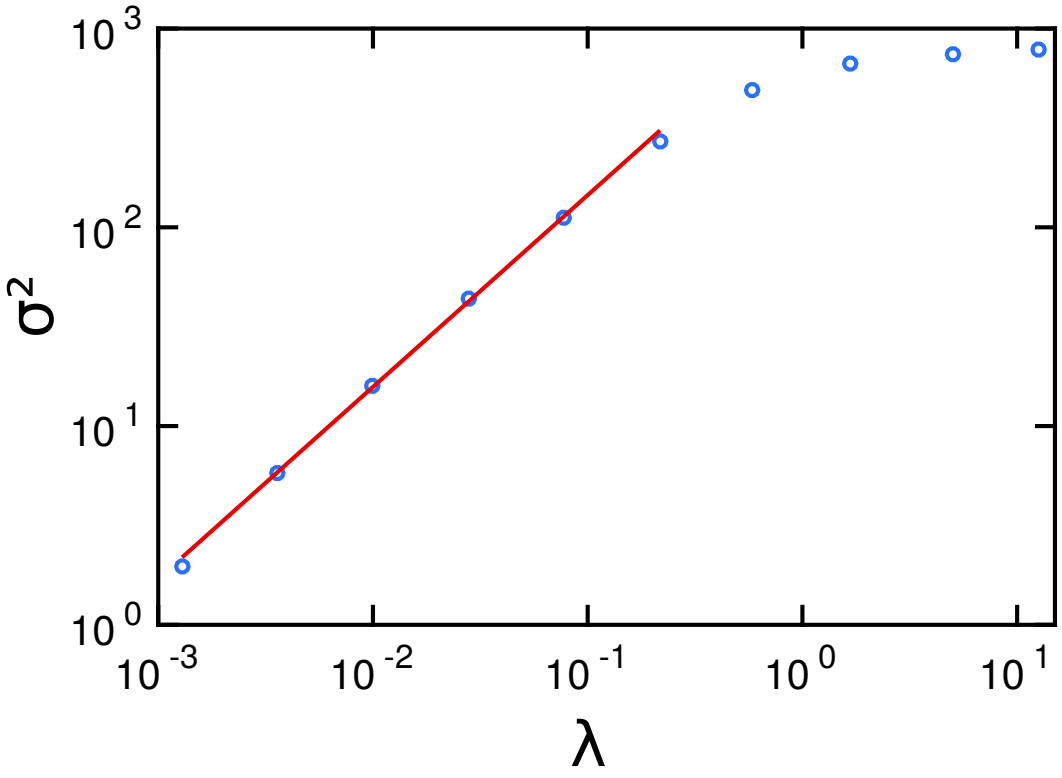

FIGURE 9. Current fluctuations as a function of mean free path
The variance of electrical current fluctuations, σ^2, is plotted against mean free path, λ. The fit is approximately linear. As the mean free path becomes large compared to the time between measurements, fluctuations asymptote to a constant value.

Probing Nonequilibrium States

Up to this point, the procedure for simulating Johnson-Nyquist noise has focused on recreating the results from the equilibrium system. However, we are primarily interested in using our model to probe nonequilibrium states in a precise and systematic manner, in particular by applying a driving force that shifts the system out of equilibrium. Subjecting the electrons to an external potential entails an input of energy into the system, disrupting the static properties of the state variables that gives rise to the equilibrium properties measured in the classical Johnson-Nyquist system.

The most straightforward way to drive the electrons out of equilibrium is to apply an external voltage, either static or time-dependent, to which the electrons will couple as they diffuse within the conductor. The electrons are coupled to the applied voltage via the Fermi surface, rather than being directly prone to the applied potential as in a vacuum. Applying a voltage shifts the Fermi surface in the direction of the applied field [59], meaning that the electrons themselves do not feel the presence of the applied voltage until they encounter a phonon and scatter to a new point on the Fermi surface dictated by the magnitude and direction of the applied voltage at that point in time. If, for example, a constant voltage is applied along the length of the conductor, the distribution of velocities in the electron gas will display a shift along the direction of the applied voltage, causing the mean velocity in that direction to be positive rather than zero, and resulting in a net flow of electrons in that direction. If the voltage is switched on at a particular time, there will be a lag between the equilibrium distribution and the new velocity distribution dictated by the mean free path of the electrons, which sets the timescale between electron interactions with the shifted Fermi surface.

In order to quantify deviations from equilibrium fluctuation-dissipation theorem in these driven states, we must define a method for extracting the values that link the perturbation to the response of the system. Turning back to the classical Johnson-Nyquist expression of the fluctuation dissipation theorem, we see that the voltage and current are random variables with a variance determined by the dissipative part of the impedance, $\overline{V^2} = \overline{I^2}R^2 = 4k_BTR$. Casting this in terms of a spectral density for the random variables allows for more thorough quantification of potential violations in the equilibrium theory. Following Kubo [4], we can define the power spectral density of fluctuations as follows:

$$G(\omega) = (1/2\pi) \int_{-\infty}^{\infty} \langle X(t_o) X(t_o + t) \rangle e^{-i\omega t} dt \tag{3.9}$$

Where $X(t)$ is the autocorrelation function of the fluctuating variable (in this case, voltage or electrical current). linear response theory dictates that for small perturbations, the admittance $\chi(\omega)$ can be written as:

$$\chi(\omega) = (\omega/2k_B T) \int_{-\infty}^{\infty} \langle A(0) A(t) \rangle e^{-i\omega t} dt \tag{3.10}$$

Where $\langle A(0)A(t) \rangle$ is the *autocorrelation function* of the observable A, in this case the voltage or current. Combining these two sides of the fluctuation-dissipation theorem gives the following:

$$G(\omega) = (2k_B T/\omega)\chi(\omega) \tag{3.11}$$

With this formulation, violations of the equilibrium fluctuation-dissipation theorem are commonly expressed as a frequency-dependent *effective temperature* that the nonequilibrium system experiences, $T \rightarrow T_{eff}(\omega)$, with $T_{eff}(\omega) = T$ indicating that the system experiences small perturbations as if it were in an equilibrium state [52]. Figure 10 shows a peak in the power spectral density that arises from a sinusoidal applied voltage, which is localized around the driving frequency in a signal which otherwise looks close to equilibrium. An effective temperature may form in this region of frequency space if the linear response function does not track the peak shown in the power spectral density.

Compared to recent experiments that probe fluctuation-dissipation in an out-of-equilibrium Johnson-Nyquist system [60], the model we have developed has the advantage of allowing the determination of both sides of the fluctuation-dissipation measurement simultaneously. Once a perturbation is applied to the system, the response function can be measured in tandem with the power spectrum of the signal as it relaxes back to equilibrium, or to a nonequilibrium state if an external potential is being applied. This simultaneous measurement can potentially unlock correlations that are obfuscated by taking measurements separately and provide insight into how a system experiences deviations from equilibrium in a controlled and continuous manner. If, for example, the linear response function tracks perturbations as they happen and follows

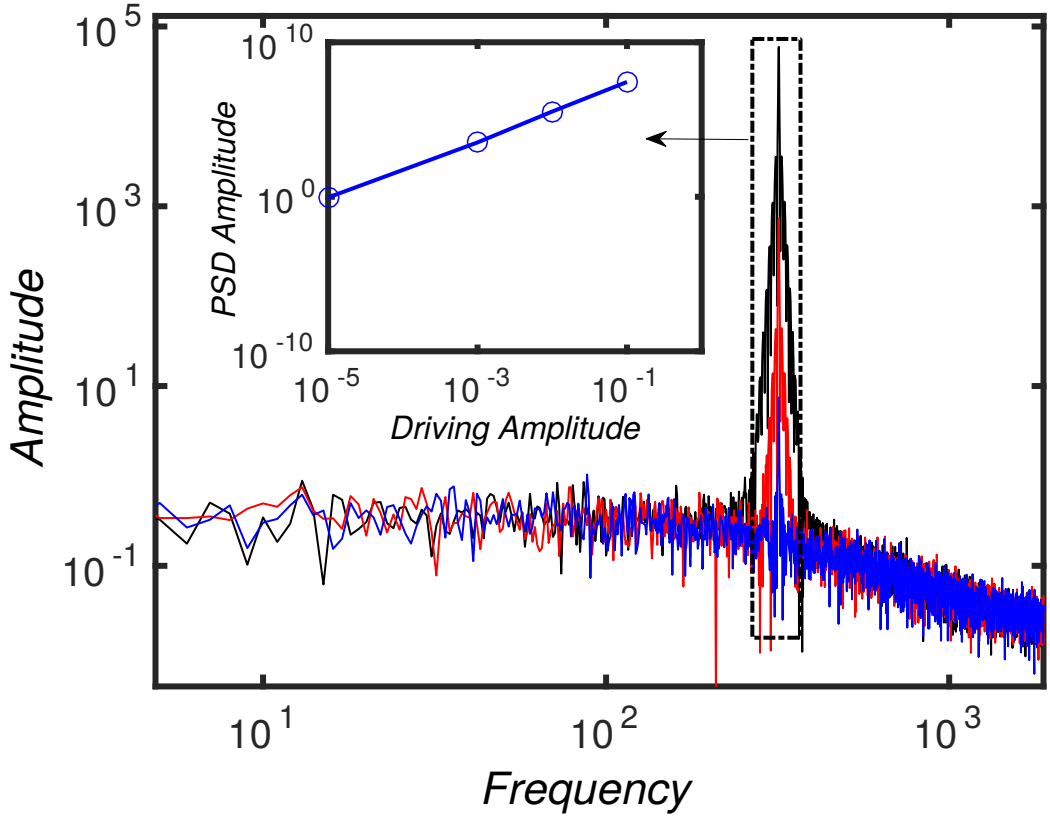

FIGURE 10. Power spectral density for driven system

Power spectral density for systems driven by a sinusoidal applied voltage. Each sinusoid has a frequency of $\omega = 1Hz$, with amplitudes $A = 0.001$ for the blue data, $A = 0.01$ for the red data, and $A = 0.1$ for the black data. The inset shows the relationship between the driving amplitude and the amplitude of the peak in the power spectral density. The first data point in the inset ($A = 0.00001$) shows the smallest value where no peak is detected in the PSD.

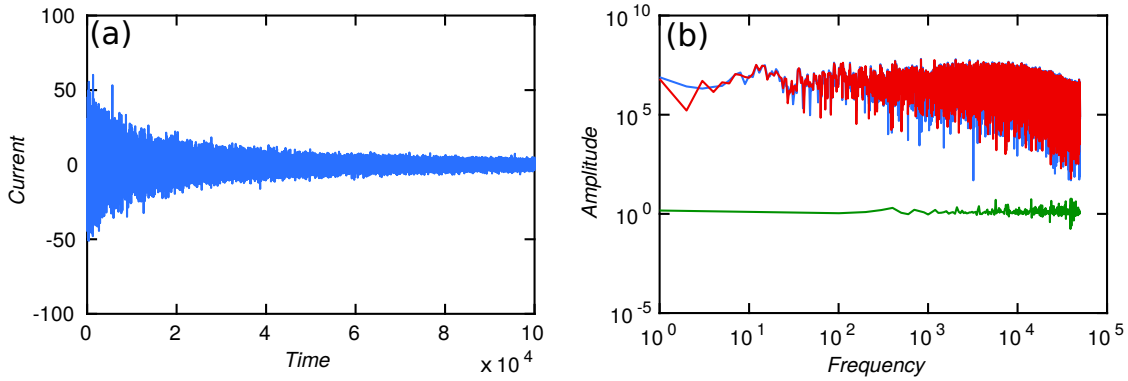

FIGURE 11. Temperature quench and effective temperature
The effect of quenching the temperature over the course of a run. (a) The fluctuating current as a function of time, showing the degree and speed of the quench. (b) The power spectral density (blue) and response function (red) of the fluctuating current, with the effective temperature (green) as a function of frequency. No deviation of the effective temperature from the equilibrium prediction is observed over the course of the run.

the power spectral density of fluctuations over time, then potential deviations that appear in both sides of the measurement may in fact not lead to an effective temperature as defined by traditional studies in nonequilibrium fluctuation-dissipation. There are also questions about how a system experiences driving forces, whether through a general increase in temperature across all frequencies, or a localized increase in only certain frequency bands. Figure 10 gives an insight into this question, as we can see that the power spectral density of fluctuations is localized around the driving frequency, while the rest of the spectrum is unaffected.

Figures 11-13 show the response of the power spectral density and response function to various types of nonequilibrium inputs. Figure 11 evaluates the system's response to a temperature quench, where the mean free path is decreased continuously over the course of the run. This involves removing energy from the system continuously over time, breaking the notion of zero energy flow between the system and environment that holds in equilibrium. Surprisingly, the temperature quench explored in Figure 11 shows no deviation from equilibrium. This is felt by the system as if it were in equilibrium, giving rise to temperature that agrees with the equilibrium prediction across all frequencies. Figures 12 and 13 show the system's response to a constant applied voltage and a sinusoidal driving voltage, respectively, each of which break equilibrium by imparting energy from the externally applied field to the system. They show deviations in the

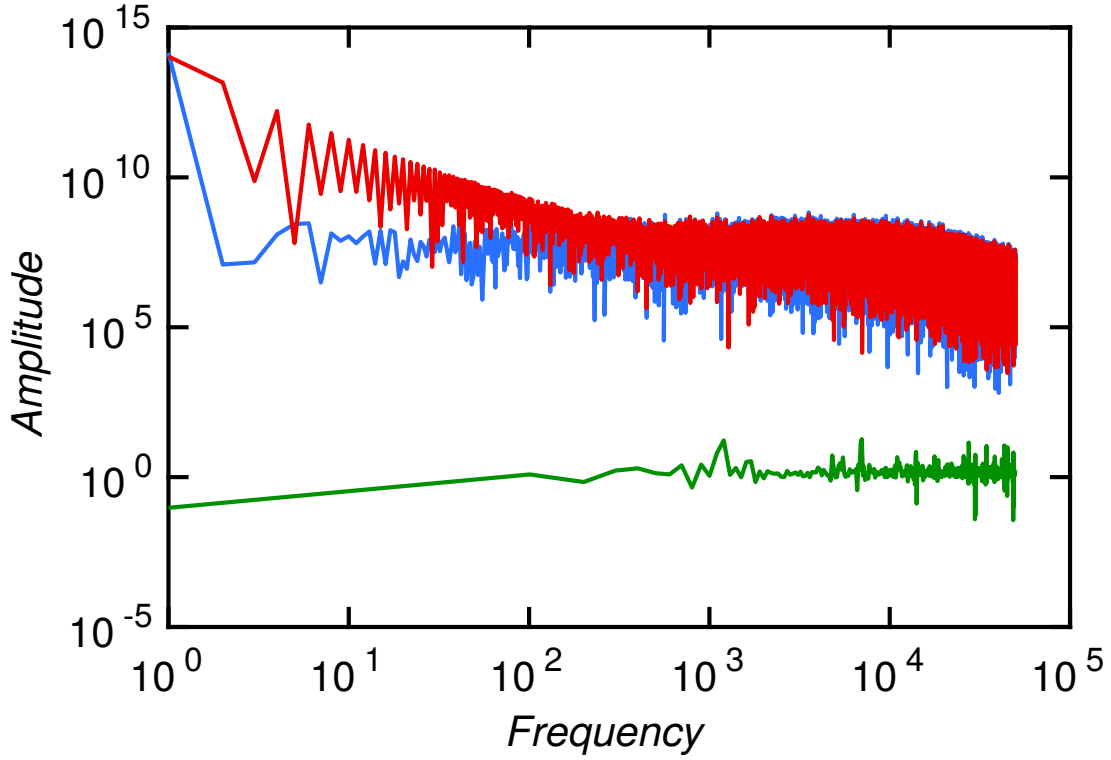

FIGURE 12. Effective temperature with constant applied voltage
The power spectral density (blue) and response function (red) of the fluctuating current, with the effective temperature (green) as a function of frequency, noise filtered for clarity. A constant voltage is applied across the conductor, resulting in a continuous average flow of current in one direction. Deviations from the equilibrium temperature are observed at low frequency but approach the equilibrium prediction at high frequency.

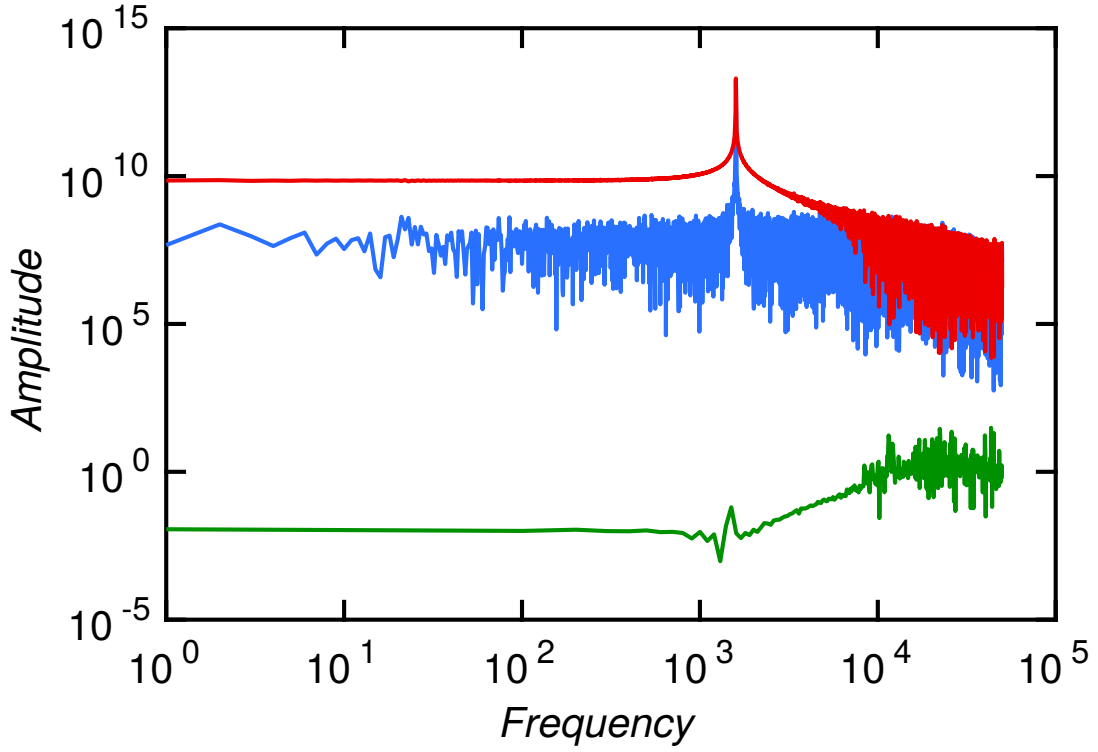

FIGURE 13. Effective temperature with sinusoidal applied voltage
The power spectral density (blue) and response function (red) of the fluctuating current, with the effective temperature (green) as a function of frequency, noise filtered for clarity. A sinusoidal voltage is applied across the conductor. Deviations from the equilibrium temperature are more complex in this case, with a spike near the driving frequency and a constant deviation at low frequency that approaches the equilibrium prediction beyond the driving frequency.

effective temperature at certain regions of frequency space, though both approach the equilibrium prediction at high frequencies.

Conclusion

We feel that it is an important first step towards better understanding the microscopic dynamics of how statistical systems behave away from equilibrium. There remains a plethora of important work to be done utilizing modern computational power in order to model statistical systems microscopically. Furthermore, establishing a working model for a system such as Johnson-Nyquist noise could help guide future experimental investigations into nonequilibrium properties of materials, as well as either corroborating or modifying the underlying theory of how the macroscopic material properties arise out of the microscopic physics. In this model, for example, we encountered an apparent inconsistency in the relationship between current fluctuations and system temperature that was unexpected at the outset. Resolving this inconsistency could lead to insights into what microscopic mechanisms drive the temperature dependence of fluctuations in the conductor, guiding future research towards a more complete picture of the electronic theory of metals.

CHAPTER IV

CONCLUSION

The work presented here has leveraged modern computational power in order to build a pair of statistical models that lend fresh insights into fundamental physical systems. Johnson-Nyquist noise and Erdős-Rényi network growth each represent momentous breakthroughs in statistical physics. In both cases, microscopic processes—electron diffusion in the case of Johnson-Nyquist noise and step-by-step connection of networks in the Erdős-Rényi case—were initially distilled down into macroscopic variables that captured the evolution of the system's state variables as observed by experiments. The explosion of computational capabilities, however, has made more thorough investigations of these processes practical and facilitated a better understanding of the underlying physics involved.

Chapter II explored a brand new model of network growth that we developed, analyzed, and published as a Rapid Communication in *Physical Review E*. In classical network growth, the high level of symmetry permits analysis of the network at any given point during its growth by simply filling a specified number of edges uniformly at random. This approach leads to state variables which evolve over time according to well-defined functions of the number of edges in the network, and thus the critical behavior of the classical percolation transition is fairly straightforward and predictable. The model developed in Chapter II follows a lineage of new growth models that exploit modern computational power by inserting evaluation algorithms into each step of the growth process. The ability to implement these evaluation algorithms requires immense computational resources as the system size grows, and our work in Chapter II makes use of the excellent resources available to us in order to simulate large systems that until recently were beyond reach.

One salient feature of the network growth process we designed in Chapter II is the ease of its implementation in real-world systems. Compared to similar processes, ours requires a minimal amount of information about the network as a whole in order to implement. In theory, the class of transitions produced by our process could be used to fluidly guide network growth in situations where delaying connectivity is desirable, and doing so would only entail collecting information about small portions of the network as any given time. There is still much to learn

and understand about these types of interventions on growing networks, and we believe that our contribution to the literature will help guide future work on designing more specialized and robust networks.

In Chapter III, the Johnson-Nyquist system of electron diffusion in a conductor was modeled using an agent-based approach to electron motion. This model treats the electrons as independent and uncorrelated from one another, scattering solely off of phonons that are generated by thermal kicks within the conductor. This model attempted to incorporate the relevant physics by distilling the factors that affect electron diffusion down into random variables pulled from the associated distributions. This entailed modeling electron scattering as a Poisson process that modifies the path of the electron according to a uniform distribution on the surface of a sphere. Surprisingly, this straightforward model does not produce the expected results, displaying an inverse relationship between temperature and the variance of current fluctuations.

There are a number of possible modifications that could be made to the simulation which may restore the proper relationship between temperature and variance of the current fluctuations. For one, the particle number is conserved across temperature for our simulations, when in fact it is possible that larger temperatures produce an increased number of free electrons. Furthermore, the resistivity of conductors is temperature dependent, and this property is not accounted for in the equilibrium Johnson-Nyquist relation, as R is static in the equation at all temperatures. It is also possible that assumptions about the probability distribution of new trajectories after a scattering event is oversimplified, and that higher temperatures lead to stronger correlations in the electron trajectory before and after scattering, which would lead to larger fluctuations for higher temperatures.

The work presented in this dissertation would not have been possible without the incredible leaps in computational power that we have experienced over the last few decades. Simulating the actions of millions of particles or choosing from among trillions of possible connections on a network feels almost trivial using modern machines. And yet, we still push up against the limit of our computing power, hoping that we can squeeze another order of magnitude into our analyses. The chasm between the macroscopic world we experience and the constituents that give rise to it is shrinking quickly, but there is still an unfathomable distance left to go. With this research, we

have taken another step towards bridging that gap, and we excitedly await the steps that will be taken in the time to come.

REFERENCES CITED

[1] Alexander J. Trevelyan, Georgios Tsekenis, and Eric I. Corwin. Degree product rule tempers explosive percolation in the absence of global information. *Physical Review E*, 97(2), feb 2018. doi: 10.1103/physreve.97.020301. URL https://doi.org/10.1103/physreve.97.020301.

[2] D. Silver, T. Hubert, J. Schrittwieser, I. Antonoglou, M. Lai, A. Guez, M. Lanctot, L. Sifre, D. Kumaran, T. Graepel, T. Lillicrap, K. Simonyan, and D. Hassabis. Mastering Chess and Shogi by Self-Play with a General Reinforcement Learning Algorithm. *ArXiv e-prints*, December 2017.

[3] H. Nyquist. Thermal agitation of electric charge in conductors. *Physical Review*, 32(1):110–113, jul 1928. doi: 10.1103/physrev.32.110. URL https://doi.org/10.1103/physrev.32.110.

[4] R Kubo. The fluctuation-dissipation theorem. *Reports on Progress in Physics*, 29(1):255–284, jan 1966. doi: 10.1088/0034-4885/29/1/306. URL https://doi.org/10.1088/0034-4885/29/1/306.

[5] Herbert B. Callen and Theodore A. Welton. Irreversibility and generalized noise. *Physical Review*, 83(1):34–40, jul 1951. doi: 10.1103/physrev.83.34. URL https://doi.org/10.1103/physrev.83.34.

[6] M. E. J. Newman. Spread of epidemic disease on networks. *Physical Review E*, 66(1), jul 2002. doi: 10.1103/physreve.66.016128. URL https://doi.org/10.1103/physreve.66.016128.

[7] H. D. Rozenfeld, L. K. Gallos, and H. A. Makse. Explosive percolation in the human protein homology network. *The European Physical Journal B*, 75(3):305–310, may 2010. doi: 10.1140/epjb/e2010-00156-8. URL https://doi.org/10.1140/epjb/e2010-00156-8.

[8] Erlend Nier, Jing Yang, Tanju Yorulmazer, and Amadeo Alentorn. Network models and financial stability. *Journal of Economic Dynamics and Control*, 31(6):2033–2060, jun 2007. doi: 10.1016/j.jedc.2007.01.014. URL https://doi.org/10.1016/j.jedc.2007.01.014.

[9] P. Gai and S. Kapadia. Contagion in financial networks. *Proceedings of the Royal Society A: Mathematical, Physical and Engineering Sciences*, 466(2120):2401–2423, mar 2010. doi: 10.1098/rspa.2009.0410. URL https://doi.org/10.1098/rspa.2009.0410.

[10] Ed Bullmore and Olaf Sporns. Complex brain networks: graph theoretical analysis of structural and functional systems. *Nature Reviews Neuroscience*, 10(3):186–198, feb 2009. doi: 10.1038/nrn2575. URL https://doi.org/10.1038/nrn2575.

[11] Won Hee Lee, Ed Bullmore, and Sophia Frangou. Quantitative evaluation of simulated functional brain networks in graph theoretical analysis. *NeuroImage*, 146:724–733, feb 2017. doi: 10.1016/j.neuroimage.2016.08.050. URL https://doi.org/10.1016/j.neuroimage.2016.08.050.

[12] Thiago Christiano Silva and Liang Zhao. *Machine Learning in Complex Networks*. Springer, 2016. ISBN 9783319172903.

[13] Steven H. Strogatz. Exploring complex networks. *Nature*, 410(6825):268–276, mar 2001. doi: 10.1038/35065725. URL https://doi.org/10.1038/35065725.

[14] Réka Albert and Albert-László Barabási. Statistical mechanics of complex networks. *Reviews of Modern Physics*, 74(1):47–97, jan 2002. doi: 10.1103/revmodphys.74.47. URL https://doi.org/10.1103/revmodphys.74.47.

[15] M. E. J. Newman. The structure and function of complex networks. *SIAM Review*, 45(2): 167–256, jan 2003. doi: 10.1137/s003614450342480. URL https://doi.org/10.1137/s003614450342480.

[16] S. N. Dorogovtsev, A. V. Goltsev, and J. F. F. Mendes. Critical phenomena in complex networks. *Reviews of Modern Physics*, 80(4):1275–1335, oct 2008. doi: 10.1103/revmodphys.80.1275. URL https://doi.org/10.1103/revmodphys.80.1275.

[17] Romualdo Pastor-Satorras, Claudio Castellano, Piet Van Mieghem, and Alessandro Vespignani. Epidemic processes in complex networks. *Reviews of Modern Physics*, 87(3): 925–979, aug 2015. doi: 10.1103/revmodphys.87.925. URL https://doi.org/10.1103/revmodphys.87.925.

[18] J. C. Doyle, D. L. Alderson, L. Li, S. Low, M. Roughan, S. Shalunov, R. Tanaka, and W. Willinger. The "robust yet fragile" nature of the internet. *Proceedings of the National Academy of Sciences*, 102(41):14497–14502, oct 2005. doi: 10.1073/pnas.0501426102. URL https://doi.org/10.1073/pnas.0501426102.

[19] R. A. da Costa, S. N. Dorogovtsev, A. V. Goltsev, and J. F. F. Mendes. Explosive percolation transition is actually continuous. *Physical Review Letters*, 105(25), dec 2010. doi: 10.1103/physrevlett.105.255701. URL https://doi.org/10.1103/physrevlett.105.255701.

[20] P. Erdős and A Rényi. On the evolution of random graphs. In *PUBLICATION OF THE MATHEMATICAL INSTITUTE OF THE HUNGARIAN ACADEMY OF SCIENCES*, pages 17–61, 1960.

[21] D. Achlioptas, R. M. D'Souza, and J. Spencer. Explosive percolation in random networks. *Science*, 323(5920):1453–1455, mar 2009. doi: 10.1126/science.1167782. URL https://doi.org/10.1126/science.1167782.

[22] Hans Hooyberghs and Bert Van Schaeybroeck. Criterion for explosive percolation transitions on complex networks. *Physical Review E*, 83(3), mar 2011. doi: 10.1103/physreve.83.032101. URL https://doi.org/10.1103/physreve.83.032101.

[23] Eric J. Friedman and Adam S. Landsberg. Construction and analysis of random networks with explosive percolation. *Physical Review Letters*, 103(25), dec 2009. doi: 10.1103/physrevlett.103.255701. URL https://doi.org/10.1103/physrevlett.103.255701.

[24] Duncan S. Callaway, John E. Hopcroft, Jon M. Kleinberg, M. E. J. Newman, and Steven H. Strogatz. Are randomly grown graphs really random? *Physical Review E*, 64(4), sep 2001. doi: 10.1103/physreve.64.041902. URL https://doi.org/10.1103/physreve.64.041902.

[25] Vikram S. Vijayaraghavan, Pierre-André Nol, Alex Waagen, and Raissa M. D'Souza. Growth dominates choice in network percolation. *Physical Review E*, 88(3), sep 2013. doi: 10.1103/physreve.88.032141. URL https://doi.org/10.1103/physreve.88.032141.

[26] Raissa M. D'Souza and Michael Mitzenmacher. Local cluster aggregation models of explosive percolation. *Physical Review Letters*, 104(19), may 2010. doi: 10.1103/physrevlett.104.195702. URL https://doi.org/10.1103/physrevlett.104.195702.

[27] Raissa M. D'Souza and Jan Nagler. Anomalous critical and supercritical phenomena in explosive percolation. *Nature Physics*, 11(7):531–538, jul 2015. doi: 10.1038/nphys3378. URL https://doi.org/10.1038/nphys3378.

[28] Y. S. Cho, B. Kahng, and D. Kim. Cluster aggregation model for discontinuous percolation transitions. *Physical Review E*, 81(3), mar 2010. doi: 10.1103/physreve.81.030103. URL https://doi.org/10.1103/physreve.81.030103.

[29] Oliver Riordan and Lutz Warnke. Explosive percolation is continuous. *Science*, 333(6040): 322–324, jul 2011. doi: 10.1126/science.1206241. URL https://doi.org/10.1126/science.1206241.

[30] Jan Nagler, Tyge Tiessen, and Harold W. Gutch. Continuous percolation with discontinuities. *Physical Review X*, 2(3), aug 2012. doi: 10.1103/physrevx.2.031009. URL https://doi.org/10.1103/physrevx.2.031009.

[31] Hans Hooyberghs, Bert Van Schaeybroeck, and Joseph O. Indekeu. Degree-dependent network growth: From preferential attachment to explosive percolation. *Physical Review E*, 89(4), apr 2014. doi: 10.1103/physreve.89.042815. URL https://doi.org/10.1103/physreve.89.042815.

[32] Alex Waagen and Raissa M. D'Souza. Given enough choice, simple local rules percolate discontinuously. *The European Physical Journal B*, 87(12), dec 2014. doi: 10.1140/epjb/e2014-50278-x. URL https://doi.org/10.1140/epjb/e2014-50278-x.

[33] Malte Schröder, S. H. Ebrahimnazhad Rahbari, and Jan Nagler. Crackling noise in fractional percolation. *Nature Communications*, 4, jul 2013. doi: 10.1038/ncomms3222. URL https://doi.org/10.1038/ncomms3222.

[34] Peter Grassberger, Claire Christensen, Golnoosh Bizhani, Seung-Woo Son, and Maya Paczuski. Explosive percolation is continuous, but with unusual finite size behavior. *Physical Review Letters*, 106(22), may 2011. doi: 10.1103/physrevlett.106.225701. URL https://doi.org/10.1103/physrevlett.106.225701.

[35] Nikolaos Bastas, Kosmas Kosmidis, and Panos Argyrakis. Explosive site percolation and finite-size hysteresis. *Physical Review E*, 84(6), dec 2011. doi: 10.1103/physreve.84.066112. URL https://doi.org/10.1103/physreve.84.066112.

[36] Raj Kumar Pan, Mikko Kivelä, Jari Saramäki, Kimmo Kaski, and János Kertész. Using explosive percolation in analysis of real-world networks. *Physical Review E*, 83(4), apr 2011. doi: 10.1103/physreve.83.046112. URL https://doi.org/10.1103/physreve.83.046112.

[37] Jan Nagler, Anna Levina, and Marc Timme. Impact of single links in competitive percolation. *Nature Physics*, 7(3):265–270, jan 2011. doi: 10.1038/nphys1860. URL https://doi.org/10.1038/nphys1860.

[38] N. Bastas, P. Giazitzidis, M. Maragakis, and K. Kosmidis. Explosive percolation: Unusual transitions of a simple model. *Physica A: Statistical Mechanics and its Applications*, 407: 54–65, aug 2014. doi: 10.1016/j.physa.2014.03.085. URL https://doi.org/10.1016/j.physa.2014.03.085.

[39] Wei Chen and Raissa M. D'Souza. Explosive percolation with multiple giant components. *Physical Review Letters*, 106(11), mar 2011. doi: 10.1103/physrevlett.106.115701. URL https://doi.org/10.1103/physrevlett.106.115701.

[40] W. Chen, Z. Zheng, and R. M. D'Souza. Deriving an underlying mechanism for discontinuous percolation. *EPL (Europhysics Letters)*, 100(6):66006, dec 2012. doi: 10.1209/0295-5075/100/66006. URL https://doi.org/10.1209/0295-5075/100/66006.

[41] Filippo Radicchi and Santo Fortunato. Explosive percolation: A numerical analysis. *Physical Review E*, 81(3), mar 2010. doi: 10.1103/physreve.81.036110. URL https://doi.org/10.1103/physreve.81.036110.

[42] *Finite-Size Scaling (Current Physics - Sources and Comments)*. North Holland, 2012.

[43] Yang-Yu Liu, Endre Csóka, Haijun Zhou, and Márton Pósfai. Core percolation on complex networks. *Physical Review Letters*, 109(20), nov 2012. doi: 10.1103/physrevlett.109.205703. URL https://doi.org/10.1103/physrevlett.109.205703.

[44] Leonard B. Loeb. *The Kinetic Theory of Gases*. Dover, 2004.

[45] Michael Plischke and Birger Bergersen. *Equilibrium statistical physics*. World Scientific, 2007.

[46] A. Einstein. Über die von der molekularkinetischen theorie der wärme geforderte bewegung von in ruhenden flüssigkeiten suspendierten teilchen. *Annalen der Physik*, 322(8):549–560, 1905. doi: 10.1002/andp.19053220806. URL https://doi.org/10.1002/andp.19053220806.

[47] H. T. Hardner, M. B. Weissman, M. B. Salamon, and S. S. P. Parkin. Fluctuation-dissipation relation for giant magnetoresistive 1/fnoise. *Physical Review B*, 48(21):16156–16159, dec 1993. doi: 10.1103/physrevb.48.16156. URL https://doi.org/10.1103/physrevb.48.16156.

[48] Johan Paulsson. Summing up the noise in gene networks. *Nature*, 427(6973):415–418, jan 2004. doi: 10.1038/nature02257. URL https://doi.org/10.1038/nature02257.

[49] A Crisanti and F Ritort. Violation of the fluctuation–dissipation theorem in glassy systems: basic notions and the numerical evidence. *Journal of Physics A: Mathematical and General*, 36(21):R181–R290, may 2003. doi: 10.1088/0305-4470/36/21/201. URL https://doi.org/10.1088/0305-4470/36/21/201.

[50] A. Barrat. Monte carlo simulations of the violation of the fluctuation-dissipation theorem in domain growth processes. *Physical Review E*, 57(3):3629–3632, mar 1998. doi: 10.1103/physreve.57.3629. URL https://doi.org/10.1103/physreve.57.3629.

[51] V. Blickle, T. Speck, C. Lutz, U. Seifert, and C. Bechinger. Einstein relation generalized to nonequilibrium. *Physical Review Letters*, 98(21), may 2007. doi: 10.1103/physrevlett.98.210601. URL https://doi.org/10.1103/physrevlett.98.210601.

[52] Ludovic Berthier and Jean-Louis Barrat. Nonequilibrium dynamics and fluctuation-dissipation relation in a sheared fluid. *The Journal of Chemical Physics*, 116(14):6228–6242, apr 2002. doi: 10.1063/1.1460862. URL https://doi.org/10.1063/1.1460862.

[53] J. Prost, J.-F. Joanny, and J. M. R. Parrondo. Generalized fluctuation-dissipation theorem for steady-state systems. *Physical Review Letters*, 103(9), aug 2009. doi: 10.1103/physrevlett.103.090601. URL https://doi.org/10.1103/physrevlett.103.090601.

[54] J. B. Johnson. Thermal agitation of electricity in conductors. *Physical Review*, 32(1):97–109, jul 1928. doi: 10.1103/physrev.32.97. URL https://doi.org/10.1103/physrev.32.97.

[55] Charles Kittel. *Elementary Statistical Physics*. Dover Publications, Mineola, N.Y, 2004. ISBN 0486435148.

[56] A. Sommerfeld and H. Bethe. Elektronentheorie der metalle. *Aufbau Der Zusammenhängenden Materie*, 1(1):333–622, jul 1933. doi: 10.1007/978-3-642-91116-3_3. URL https://doi.org/10.1007/978-3-642-91116-3_3.

[57] D. L. Rode and S. Knight. Electron transport in GaAs. *Physical Review B*, 3(8):2534–2541, apr 1971. doi: 10.1103/physrevb.3.2534. URL https://doi.org/10.1103/physrevb.3.2534.

[58] V. L. Moruzzi, J. F. Janak, and K. Schwarz. Calculated thermal properties of metals. *Physical Review B*, 37(2):790–799, jan 1988. doi: 10.1103/physrevb.37.790. URL https://doi.org/10.1103/physrevb.37.790.

[59] H Ibach. *Solid-State Physics: An Introduction to Principles of Materials Science*. Springer, Berlin New York, 2009. ISBN 3540938036.

[60] N. Garnier and S. Ciliberto. Nonequilibrium fluctuations in a resistor. *Physical Review E*, 71 (6), jun 2005. doi: 10.1103/physreve.71.060101. URL https://doi.org/10.1103/physreve.71.060101.